

Coulomb-assisted nonlocal electron transport between two pairs of Majorana bound states in a superconducting island

Hao-Di Wang(王浩迪), Jun-Tong Ren(任俊潼), Hai-Feng Lü(吕海峰), and Sha-Sha Ke(柯莎莎)

Citation: Chin. Phys. B, 2024, 33 (**5**): 050310. DOI: 10.1088/1674-1056/ad2a68
Journal homepage: http://cpb.iphy.ac.cn; http://iopscience.iop.org/cpb

What follows is a list of articles you may be interested in

Recurrent neural network decoding of rotated surface codes based on distributed strategy

Fan Li(李帆), Ao-Qing Li(李熬庆), Qi-Di Gan(甘启迪), and Hong-Yang Ma(马鸿洋)
Chin. Phys. B, 2024, 33 (**4**): 040307. DOI: 10.1088/1674-1056/ad2bef

Dilation, discrimination and Uhlmann's theorem of link products of quantum channels

Qiang Lei(雷强), Liuheng Cao(操刘桁), Asutosh Kumar, and Junde Wu(武俊德)
Chin. Phys. B, 2024, 33 (**3**): 030304. DOI: 10.1088/1674-1056/ad0ccb

Unconventional photon blockade in the two-photon Jaynes-Cummings model with two-frequency cavity drivings and atom driving

Xin Liu(刘欣), Meng-Yu Tian(田梦雨), Xiao-Ning Cui(崔晓宁), and Xin-He Zhang(张馨鹤)
Chin. Phys. B, 2024, 33 (**2**): 020308. DOI: 10.1088/1674-1056/ad0cca

Quantum synchronization with correlated baths

Lei Li(李磊), Chun-Hui Wang(王春辉), Hong-Hao Yin(尹洪浩), Ru-Quan Wang(王如泉), and Wu-Ming Liu(刘伍明)
Chin. Phys. B, 2024, 33 (**2**): 020306. DOI: 10.1088/1674-1056/ad0bef

Detection of spin current through a quantum dot with Majorana bound states

Ning Wang(王宁), Xingtao An(安兴涛), and Shuhui Lv(吕树慧)
Chin. Phys. B, 2021, 30 (**10**): 100302. DOI: 10.1088/1674-1056/abff1c

---

Coulomb-assisted nonlocal electron transport between two pairs of Majorana bound states in a superconducting island

Hao-Di Wang(王浩迪), Jun-Tong Ren(任俊潼), Hai-Feng Lü(吕海峰)[†], and Sha-Sha Ke(柯莎莎)[‡]

School of Physics, University of Electronic Science and Technology of China, Chengdu 610054, *China*

(Received 26 September 2023; revised manuscript received 24 January 2024; accepted manuscript online 19 February 2024)

We investigate the nonlocal transport modulated by Coulomb interactions in devices comprising two interacting Majorana wires, where both nanowires are in proximity to a mesoscopic superconducting (SC) island. Each Majorana bound state (MBS) is coupled to one lead via a quantum dot with resonant levels. In this device, the nonlocal correlations can be induced in the absence of Majorana energy splitting. We find that the negative differential conductance and giant current noise cross correlation could be induced, due to the interplay between nonlocality of MBSs and dynamical Coulomb blockade effect. This feature may provide a signature for the existence of the MBSs.

Keywords: Majorana bound states, superconducting island, current cross correlation

PACS: 03.75.Lm, 72.10.–d, 74.78.Na, 73.21.La **DOI:** 10.1088/1674-1056/ad2a68

1. Introduction

One of the most influential recent discoveries is that topological phases supporting Majorana fermions can be realized and engineered in the heterostructures based on s-wave superconductors and materials with strong spin–orbit interaction.[1] The search of Majorana bound states (MBSs) is motivated in part by their potential application in fault-tolerant computation due to their non-Abelian characteristics.[2–5] Experimental efforts to implement the nanowire proposal have uncovered evidence for a zero bias peak in tunneling spectroscopy studies of hybrid superconductor-semiconductor devices.[6–14] Despite suggestive observations, however, unambiguous experimental verification remains elusive because zero-bias peaks can also result from non-Majorana sources.[15–25]

The signal of current noise cross correlation (CC) could provide a confirmative proof to check existence of MBSs. In non-Majorana devices, it has been experimentally demonstrated that Cooper pairs can be split into spin-entangled electrons flowing in two spatially separated normal metals, resulting in a positive current–current correlation.[26–31] Although there are many theoretical studies devoted to investigate the property of noise CC induced by MBSs,[32–39] the Majorana-modulated nonlocal transport has not been reported up to date. One of the possible reasons is that the Majorana energy splitting, which is essential to induce the noise CC, is generally weak and approaches to zero in some cases. Typical values of Majorana energy splitting is only about 0 to several 10 μeV in a topological nanowire with its length 1–2 μm.[40–42] This is much weaker than other mechanisms that also induce current–current correlations, such as intra- and inter-dot Coulomb interaction[43–45] and superconducting (SC) pairing energy.[26–28,30] Therefore, it is highly desirable to produce stronger current–current correlation by combining the nonlocality of MBSs and other robust physical mechanisms, instead by Majorana energy splitting.

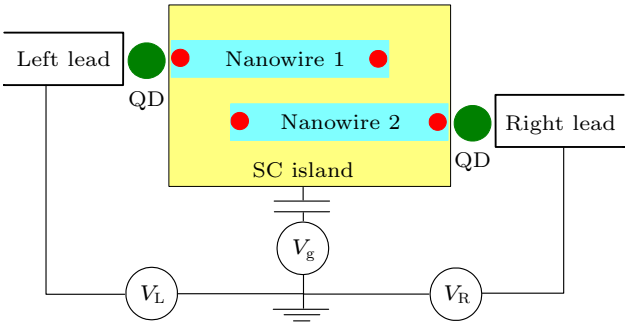


Fig. 1. Scheme view of the device. Two Majorana nanowires are proximity-coupled to a mesoscopic SC island with a finite charging energy. Under proper magnetic field, the nanowires are driven into the topological phase and a pair of MBSs appear in the wire ends. One end of each nanowire is connected to a quantum dot and a normal metal lead. Crossed Andreev reflection can be detected by correlating the currents that flow into two topological nanowires via MBSs. In the presence of the charging energy in the island, nonlocal current cross correlation could be generated for zero Majorana energy splitting.

2. Model and formula

Here we propose a scheme to generate robust nonlocal current noise CC in a Coulomb–Majorana device, where a finite Majorana energy splitting is not essential. Schematic setup of the multiterminal Coulomb–Majorana junction is illustrated in Fig. 1: Considering two semiconductor nanowires proximity-coupled to the same mesoscopic SC island with a finite charging energy U_0, there exist two pairs of MBSs under proper magnetic field.[1] One end of each nanowire connects to a quantum dot and a normal metal lead. It is convenient to define nonlocal auxiliary fermion operators $\eta_{ja} = f_j + f_j^\dagger$ and $\eta_{jb} = \mathrm{i}(f_j^\dagger - f_j)$ $(j = 1, 2)$ for MBSs, with total number oper-

[†]Corresponding author. E-mail: lvhf04@uestc.edu.cn
[‡]Corresponding author. E-mail: keshasha@uestc.edu.cn

© 2024 Chinese Physical Society and IOP Publishing Ltd

ator $\hat{n}_f = f_1^\dagger f_1 + f_2^\dagger f_2$. In the regular fermion representation, the instantaneous charge state of the SC island is expressed by (N_C, n_{f1}, n_{f2}), where the integer N_C represents the Cooper pair number operator in the island and n_{fj} is eigenvalues of $\hat{n}_{fj}$, respectively. Including the Majorana energy splitting and a Coulomb charging term, the Hamiltonian of the SC island reads[46]

$$H_w = \sum_j \varepsilon_j f_j^\dagger f_j + E_C(2\hat{N}_C + \hat{n}_{f1} + \hat{n}_{f2} - n_g)^2, \tag{1}$$

where the intra-island capacitive charging effect energy E_C can be tuned by a gate voltage parameter $n_g \propto V_g$. In a realistic experiment, the typical value of E_C is about 100 μeV.[47,48] Furthermore, the Josephson tunneling E_J between the island the the bulk superconductor is expressed as

$$H_J = -E_J \cos\varphi = -\frac{E_J}{2}(e^{i\varphi} + e^{-i\varphi}), \tag{2}$$

where the operator $e^{i\varphi}$ ($e^{-i\varphi}$) raises (lowers) the Cooper pair number by one unit, $N_C \rightharpoonup N_C \pm 1$.

The topological charge of the island that contains two pairs of MBSs equals the fermion parity

$$\mathcal{P} = -\eta_{1a}\eta_{1b}\eta_{2a}\eta_{2b} = (2n_{f1} - 1)(2n_{f2} - 1). \tag{3}$$

The eigenvalues of $\mathcal{P}$ are ± 1, depending on whether there is an even or an odd number of electrons on the island. We focus on the transport property in the Josephson regime $E_J \gg E_C$. In this regime, the effective low-energy Hamiltonian describing the SC island could be derived as

$$H_{\text{eff}} = -E_J + \sqrt{2E_C E_J} - U_0\mathcal{P} + \sum_j \varepsilon_j f_j^\dagger f_j, \tag{4}$$

where

$$U_0 = 16(E_C E_J^3/2\pi^2)^{1/4} e^{-\sqrt{8E_J/E_C}} \cos(\pi n_g). \tag{5}$$

It is noted that both the sign and the strength of the interaction parameter U_0 can be tuned continuously by n_g. By ignoring the constant term, the effective model Hamiltonian of the device in the central region is given by

$$\begin{aligned} H_c = &\sum_{j=1,2} (\varepsilon_j d_j^\dagger d_j + \varepsilon_{Mj} f_j^\dagger f_j) - U_0(2n_{f1} - 1)(2n_{f2} - 1) \\ &+ \lambda_1(d_1^\dagger - d_1)(f_1^\dagger + f_1) + \lambda_2(f_2^\dagger - f_2)(d_2^\dagger + d_2), \end{aligned} \tag{6}$$

where $d_j^\dagger$ and $f_j^\dagger$ ($j = 1, 2$) are respectively the creation operators for electrons in dot j and MBS j; ε_{Mj} denotes the Majorana energy splitting, λ_j represents the dot–Majorana coupling strength, and ε_j is the energy level of the dot j. The dot–lead tunneling Hamiltonian is given by $H_t = \sum_{jk}(t_j a_{jk}^\dagger d_j + \text{h.c.})$, where t_j is the dot-lead coupling strength and $a_{jk}^\dagger$ represents the creation operator of an electron on lead j.

We take the diagonalized master equation (DME) approach to investigate the electronic transport through this system in the sequential regime.[49–54] In the DME approach, we firstly diagonalize the Hamiltonian H_c of the central region and obtain the eigenvalues E_n and their corresponding eigenfunctions $|\beta_n\rangle$. In the Born–Markov approximation, the time evaluation of the density matrix $\rho_D(t) = |\beta_n\rangle\langle\beta_{n'}|$ of the states $|\beta_n\rangle$ is given by the rate equation

$$\frac{d}{dt}\rho_D(t) = \boldsymbol{W}\rho_D(t), \tag{7}$$

where elements of the rate matrix are the same as given in Refs. [36,53], $W_{n'n} = \sum_i (W_{n'n}^{i+} + W_{n'n}^{i-})$ for $n \neq n'$ and $W_{nn} = -\sum_{n' \neq n}^N W_{n'n}$. The coefficient $W_{n'n}^{i+} = \Gamma_i f(\Delta_{n'n} + \mu_i)|\langle\beta_{n'}|d_i|\beta_n\rangle|^2$ and $W_{n'n}^{i-} = \Gamma_i f(\Delta_{n'n} - \mu_i)|\langle\beta_{n'}|d_i^\dagger|\beta_n\rangle|^2$ denote the rates for a transition $|\beta_n\rangle \to |\beta_{n'}\rangle$ by adding or annihilating an electron in dot i, with $\Gamma_i = 2\pi|t_i|^2\rho_i$ being the bare electronic tunneling rate (ρ_i the density of states of lead i), $f_i(\omega) = [1 + e^{\omega/k_B T}]^{-1}$ the Fermi distribution function, μ_i the chemical potential in lead i, and $\Delta_{n'n}$ the Bohr frequency of the transition from $|\beta_n\rangle$ to $|\beta_{n'}\rangle$.

Within the DME approach, the current I_i can be written as $I_i = e\sum_n[\hat{\boldsymbol{I}}^i\rho_D]_n$, where $\hat{\boldsymbol{I}}^i$ is the matrix of the current operator and its element is given by $\hat{I}_{n'n}^i = W_{n'n}^{i-} - W_{n'n}^{i+}$. The noise power spectra can be expressed as the Fourier transform of the current–current correlation function

$$S_{I_i I_j}(\omega) = 2\langle I_i(t) I_j(0)\rangle_\omega - 2\langle I_i\rangle_\omega\langle I_j\rangle_\omega. \tag{8}$$

Here I_i and I_j are the electrical currents across the i and j junctions, and t is the time. Furthermore, the current–current correlation in the ω-space becomes $\langle I_i(t)I_j(0)\rangle_\omega = \sum_k[\hat{I}^i\hat{T}(\omega)\hat{I}^j\boldsymbol{\rho}^{(0)} + \hat{I}^j\hat{T}(-\omega)\hat{I}^i\boldsymbol{\rho}^{(0)}]_k$, where $\hat{T}(\pm\omega) = (\mp i\omega\hat{I} - \boldsymbol{W})^{-1}$.

The transport properties in the device with a single pair of MBSs has been widely studied.[32–38] In the absence of Coulomb interaction, it has been shown that the DME works well in most regimes of system parameters compared with the exact solution.[55] Nevertheless, the results of the DME approach show a clear deviation in the current correlation for strong dot–lead coupling strength or when energy degeneracy appears in the central region. Except for current correlations in these special cases, the transport properties obtained from DME approach are in agreement well with the exact solution by using the nonequilibrium Green's function method, which ensures us to apply the DME approach to more general interacting cases that can not be exactly solved.

3. Results and discussion

In most previous references, nonlocal communication of a Majorana system is generated based on a finite Majorana energy splitting ε_M.[32–38] In the noninteracting case, nonlocal communication vanishes for $\varepsilon_M = 0$. Here it is expected that the Coulomb interaction U_0 could induce the nonlocal correlation between two tunneling pathes for vanishing Majorana energy splitting, i.e., $\varepsilon_{M1} = \varepsilon_{M2} = 0$. The effect of Coulomb interaction in the SC island on transport properties is illustrated in

Fig. 2. In the absence of Coulomb interaction ($U_0 = 0$), there is no correlation between two tunneling pathes and $S_{12} = 0$. The system is decoupled two separated Majorana–dot devices, and its transport property has been widely investigated in several earlier references.[56–58] Compared to the noninteracting and exactly solvable cases, an important difference in the transport is that the Coulomb interaction could induce a negative differential conductance (NDC), as shown in Fig. 2(a). With the increase of lead voltage from $V_0 = 0$, the current appears and increases gradually when the voltage scans through the lowest positive eigenenergy of the central region. However, as the lead voltage increases and other energy levels lie in the transport window, the Coulomb interaction induces strong competition between different tunneling pathes, leading to decrease of current. The behavior similar to that of the current can be also observed in the voltage dependence of the noise CC [see Fig. 2(b)]. S_{12} is strongly enhanced in the transport regime where the system is in the NDC regime.

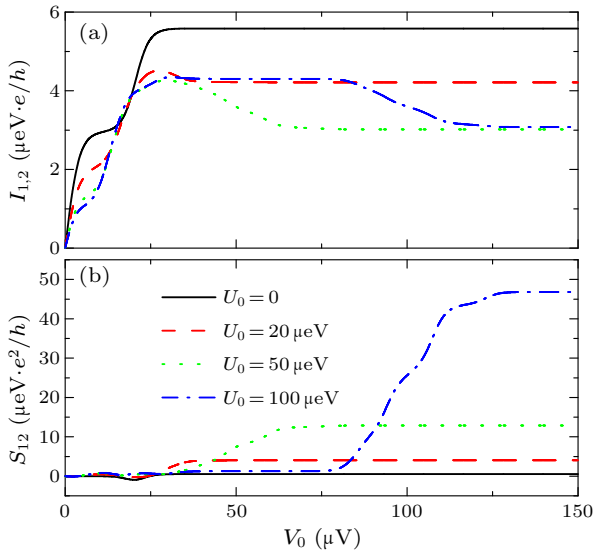


Fig. 2. (a) Current $I_{1,2}$ and (b) zero-frequency cross correlation S_{12} versus lead voltage V_0 for different Coulomb interactions $U_0 = 0$, 20 μeV, 50 μeV, and 100 μeV. Other parameters: $k_BT = 2$ μeV, $\varepsilon_{1,2} = 5$ μeV, $\varepsilon_{M1,M2} = 0$ μeV, $\lambda_{1,2} = 10$ μeV, and $\Gamma_0 = 1$ μeV.

The physics of the giant noise CC originates from the combined effects of Coulomb blockade and nonlocality of MBSs, and can be understood by considering the time-dependent dynamics of the system. For small lead voltages, the thermal-activated current dominates and the current–current correlations mainly governed by dynamical charge fluctuations. Due to the inter-Majorana Coulomb interaction, the degeneracy for the Majorana–dot device is lifted and the eigenenergies become Coulomb dependent. This dependence remarkably modifies the electronic occupation behavior in comparison with the no shifting case. The system have more opportunity to occupy the one state for large bias voltages, leading to a decrease of the occupation number of other states with increasing bias voltage. For high lead voltage, the highest-energy eigenstate of H_c enters the transport window, but it is coupled to electronic reservoirs weakly. Typically, the system spends a long time in this state before a transition takes place, resulting the inter-channel blockade. In this regime the crossed Andreev reflection begins to play an essential role. Strong polarization fluctuations are activated and they yield a positive contribution to S_{12}, which becomes dominating and results in giant CC. The dynamical channel blockade is also demonstrated in various systems, such as in multilevel quantum dot devices[59–64] and Franck–Condon blockade in single molecules[65] and nanoscale oscillators.[66]

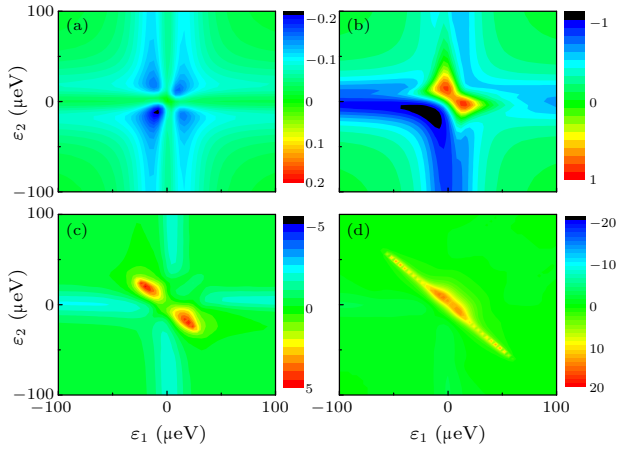


Fig. 3. Coulomb interaction induced zero-frequency current noise cross correlation S_{12} versus dot energy levels ε_1 and ε_2 for different voltages: (a) $V_0 = 2$ μV, (b) 10 μV, (c) 30 μV, and (d) 60 μV. Other parameters: $U_0 = 50$ μeV, $\varepsilon_{M1} = 2$ μeV, $\varepsilon_{M2} = 1$ μeV, $k_BT = 2$ μeV, $\lambda_{1,2} = 10$ μeV, and $\Gamma_0 = 1$ μeV.

The insertion of quantum dots not only modulates the sign of current CC, but also provides a way to distinct from CC in the absence of MBSs.[36–38] In Fig. 3 we demonstrate the noise CC S_{12} as a function of dot energy levels ε_1 and ε_2 for different lead voltages V_0. It is shown that in different lead voltage regimes, the current CC indicates distinct correlation patterns. With the increase of V_0, S_{12} is considerably enhanced, especially in the large voltage regime. For a small V_0, the currents are mainly contributed by thermal activation, and four sets of sectors with negative S_{12} are formed with an L-shape pattern. This negative four-sector correlation pattern is quite different from those induced by Majorana energy splitting, in which a four-peaked clover-like pattern is formed with two negative and two positive regions.[36–38] With the increase of V_0, more and more eigenstates with positive energies enter the transport window and positive S_{12} appears in the regions of ($\varepsilon_1 > 0$, $\varepsilon_2 < 0$) and ($\varepsilon_1 < 0$, $\varepsilon_2 > 0$). With increasing V_0 further, the thermal fluctuation effect is suppressed, while the CC caused by competition between different eigenstates is dominant gradually. In the large V_0 regime, the large CC appears, while the negative correlation is weakened. The positive CC is mainly distributed along the line of asymmetric dot level configuration ($\varepsilon_1 = -\varepsilon_2$).

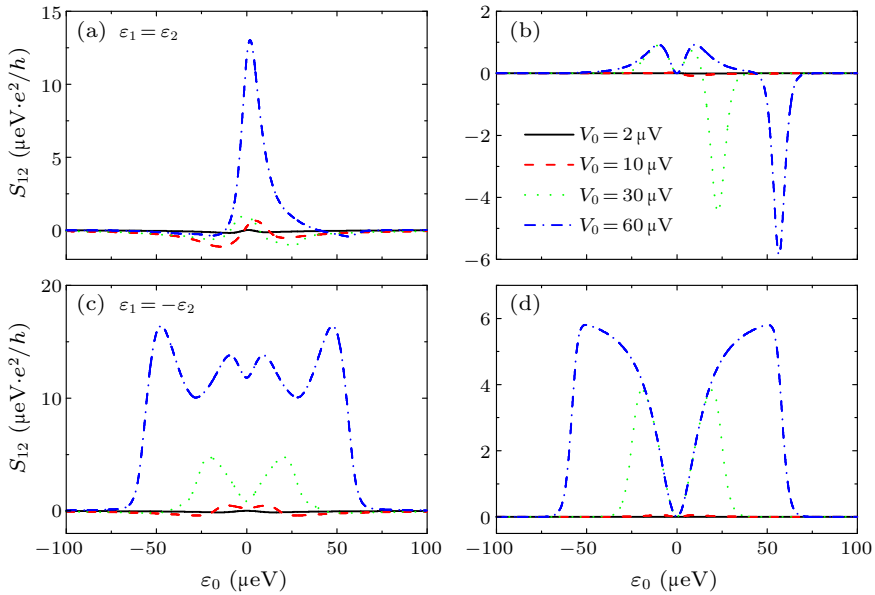


Fig. 4. Coulomb interaction induced current noise cross correlation S_{12} as functions of (a) symmetric dot energy level ε_0 ($=\varepsilon_1=\varepsilon_2$) and (c) antisymmetric dot energy level ε_0 ($=\varepsilon_1=-\varepsilon_2$) for different voltages $V_0=2$ μV, 10 μV, 30 μV, and 60 μV, where $U_0=50$ μeV and $\lambda_0=0$. Majorana energy splitting induced S_{12} for the cases (b) $\varepsilon_1=\varepsilon_2$ and (d) $\varepsilon_1=-\varepsilon_2$, where $U_0=0$ and $\lambda_0=5$ μeV. Other parameters: $\varepsilon_{Mi}=2$ μeV, $k_BT=2$ μeV, $\lambda_i=10$ μeV, and $\Gamma_0=1$ μeV.

Except for the Coulomb interaction, the direct coupling between MBSs in two nanowires could also induce current CC. In order to distinguish the difference in CC caused by these two mechanisms, we introduce the direct MBSs coupling $H_d=-i\lambda_0\eta_{1b}\eta_{2a}$, where λ_0 is the coupling strength. In Fig. 4 we illustrate the noise CC S_{12} induced by Coulomb interaction in the SC island and direct coupling between two paired MBSs, respectively. We separately consider the symmetric dot level configurations with $\varepsilon_1=\varepsilon_2=\varepsilon_0$ and antisymmetric configuration with $\varepsilon_1=-\varepsilon_2=\varepsilon_0$. For different lead voltages, these two mechanisms modulate the CC in a similar rule. In the case of symmetric level configuration $\varepsilon_1=\varepsilon_2$, S_{12} indicates sign reversals as a function of dot energy level. For small lead voltage, negative S_{12} is favorable to be induced. With the increase of V_0, the Coulomb interaction enhances the positive CC when the dot levels lie in the middle position of the superconducting gap, while the Majorana energy splitting mainly enhances the negative S_{12} for $\varepsilon_i\sim V_i$. In the large voltage regime, Coulomb interaction could generate large noise CC by dynamical inter-channel blockade effect. For the antisymmetric configuration $\varepsilon_1=-\varepsilon_2$, the direct coupling λ_0 between MBSs induces only positive S_{12} and the CC is symmetric as a function of dot energy level, as a manifest of the particle-hole symmetry. In the noninteracting case, effect of the direct tunneling between two Majorana wires is to renormalize the total Majorana energy splitting. In the case of antisymmetric level configuration, Majorana energy splitting only induces positive CC,[36–38] which is consistent with the results shown in Fig. 4(d). Differently, the Coulomb interaction induces negative CC when a small lead voltage is applied for $\varepsilon_1=-\varepsilon_2$. Similar to the symmetric level configuration, the Coulomb interaction strongly enhances S_{12} with the increase of V_0, and in the large lead voltage, a huge S_{12} can be induced.

4. Conclusions

We have investigated the Coulomb-mediated nonlocal transport in a device comprising of two Majorana nanowires in proximity to a mesoscopic SC island, in which each nanowire is weakly connected to one quantum dot and one normal metal lead. We show that the proposed device leads to interesting physics including the occurrence of NDC and large current noise CC, arising from the interplay between Majorana's nonlocality and dynamical inter-channel blockade effect. The feature of interaction induced nonlocal communication in a Majorana setup is quite different from current CC caused by Majorana energy splitting. It is expected that our proposal provides a more feasible scheme to confirm existence of Majorana fermions.

Acknowledgements

This work was supported by the National Natural Science Foundation of China (Grant Nos. 12074209 and 12274063), the Fundamental Research Funds for the Central Universities (Grant No. ZYGX2019J100), and the Open Project of State Key Laboratory of Low-Dimensional Quantum Physics (Grant No. KF202008).

References

[1] Beenakker C W J 2013 *Annu. Rev. Condens. Matter Phys.* **4** 113
[2] Nayak C, Simon S H, Stern A, Freedman M and Das Sarma S 2008 *Rev. Mod. Phys.* **80** 1083
[3] Stern A 2010 *Nature* **464** 187
[4] Fu L 2010 *Phys. Rev. Lett.* **104** 056402
[5] Flensberg K 2011 *Phys. Rev. Lett.* **106** 090503

[6] Wang Z, Rodriguez J O, Jiao L, Howard S, Graham M, Gu G D, Hughes T L, Morr D K and Madhavan V 2020 *Science* **367** 104
[7] Prada E, San-Jose P, de Moor M W A, Geresdi A, Lee E J H, Klinovaja J, Loss D, Nygård J, Aguado R and Kouwenhoven L P 2020 *Nat. Rev. Phys.* **2** 575
[8] Flensberg K, von Oppen F and Stern A 2021 *Nat. Rev. Mater.* **6** 944
[9] Ren H, Pientka F, Hart S, *et al.* 2019 *Nature* **569** 93
[10] Fornieri A, Whiticar A M, *et al.* 2019 *Nature* **569** 89
[11] Vaitiekenas S, Liu Y, Krogstrup P and Marcus C M 2021 *Nat. Phys.* **17** 43
[12] Crawford D, Mascot E, Shimizu M, Beck P, Wiebe J, Wiesendanger R, Jeschke H O, Morr D K and Rachel S 2022 *npj Quantum Mater.* **7** 117
[13] Chen J, Xu W, Tan Z, Pan Z, Zhu P, Liao Z M and Yu D 2022 *Nano Lett.* **22** 6484
[14] Li M, Li G, Cao L, Zhou X, Wang X, Jin C, Chiu C K, Pennycook S J, Wang Z and Gao H J 2022 *Nature* **606** 890
[15] Sau J D and Brydon P M R 2015 *Phys. Rev. Lett.* **115** 127003
[16] Moore C, Zeng C, Stanescu T D and Tewari S 2018 *Phys. Rev. B* **98** 155314
[17] Woods B D, Das Sarma S and Stanescu T D 2021 *Phys. Rev. Appl.* **16** 054053
[18] Ahn S, Pan H, Woods B, Stanescu T D and Das Sarma S 2021 *Phys. Rev. Mater.* **5** 124602
[19] Pan H, Liu C-X, Wimmer M and Das Sarma S 2021 *Phys. Rev. B* **103** 214502
[20] Frolov S 2021 *Nature* **592** 350
[21] Valentini M, Peñaranda F, Hofmann A, Brauns M, Hauschild R, Krogstrup P, San-Jose P, Prada E, Aguado R, and Katsaros G 2021 *Science* **373** 82
[22] Hess R, Legg H F, Loss D and Klinovaja J 2021 *Phys. Rev. B* **104** 075405
[23] Yu P, Chen J, Gomanko M, Badawy G, Bakkers E P A M, Zuo K, Mourik V and Frolov S M 2021 *Nat. Phys.* **17** 482
[24] Das Sarma S and Pan H 2021 *Phys. Rev. B* **103** 195158
[25] Pan H and Das Sarma S 2022 *Phys. Rev. B* **105** 115432
[26] Hofstetter L, Csonka S, Nygård J and Schönenberger C 2009 *Nature* **461** 960
[27] Hofstetter L, Csonka S, Baumgartner A,, *et al.* 2011 *Phys. Rev. Lett.* **107** 136801
[28] Wei J and Chandrasekhar V 2012 *Nat. Phys.* **6** 494
[29] Min J H, Lee K, Chung T H, *et al.* 2022 *Opto-Electron. Sci.* **1** 220016
[30] Das A, Ronen Y, Heiblum M, Mahalu D, Kretinin A V and Shtrikman H 2012 *Nat. Commun.* **3** 1165
[31] Huang H J, Balcytis A, Dubey A, *et al.* 2023 *Opto-Electron. Sci.* **2** 220022
[32] Bolech C J and Demler E 2007 *Phys. Rev. Lett.* **98** 237002
[33] Nilsson J, Akhmerov A R and Beenakker C W J 2008 *Phys. Rev. Lett.* **101** 120403
[34] Tewari S, Zhang C, Das Sarma S, Nayak C and Lee D H 2008 *Phys. Rev. Lett.* **100** 027001
[35] Law K T, Lee P A and Ng T K 2009 *Phys. Rev. Lett.* **103** 237001
[36] Lü H F, Lu H Z and Shen S Q 2012 *Phys. Rev. B* **86** 075318
[37] Zocher B and Rosenow B 2013 *Phys. Rev. Lett.* **111** 036802
[38] Liu J, Zhang F C and Law K T 2013 *Phys. Rev. B* **88** 064509
[39] Porfirev A, Khonina S, Ustinov A, Ivliev N and Golub I 2023 *Opto-Electron. Sci.* **2** 230014
[40] Das Sarma S, Sau J D and Stanescu T D 2012 *Phys. Rev. B* **86** 220506
[41] Chen J Y, Eul T, Lyu L, *et al.* 2022 *Opto-Electron. Sci.* **1** 210011
[42] Yan S Q, Zuo Y, Xiao S S, Oxenlowe L K and Ding Y H 2022 *Opto-Electron. Adv.* **5** 210159
[43] McClure D T, DiCarlo L, Zhang Y, *et al.* 2007 *Phys. Rev. Lett.* **98** 056801
[44] Zhang Y, DiCarlo L, McClure D T, Yamamoto M, Tarucha S, Marcus C M, Hanson M P and Gossard A C 2007 *Phys. Rev. Lett.* **99** 036603
[45] Liu S Q, Chen S Z, Wen S C and Luo H L 2022 *Opto-Electron. Sci.* **1** 220007
[46] Hützen R, Zazunov A, Braunecker B, Yeyati A L and Egger R 2012 *Phys. Rev. Lett.* **109** 166403
[47] Sillanpää M A, Lehtinen T, Paila A, Makhlin Yu, Roschier L and Hakonen P J 2005 *Phys. Rev. Lett.* **95** 206806
[48] Naaman O and Aumentado J 2007 *Phys. Rev. Lett.* **98** 227001
[49] Bruus H and Flensberg K 2004 *Many-Body Quantum Theory in Condensed Matter Physics* (Oxford: Oxford University Press)
[50] Kashcheyevs V, Aharony A and Entin-Wohlman O 2006 *Phys. Rev. B* **73** 125338
[51] Mitra A and Millis A J 2007 *Phys. Rev. B* **76** 085342
[52] Timm C 2008 *Phys. Rev. B* **77** 195416
[53] Pöltl C, Emary C and Brandes T 2009 *Phys. Rev. B* **80** 115313
[54] Lu H Z, Zhou B and Shen S Q 2009 *Phys. Rev. B* **79** 174419
[55] Lü H F, Lu H Z and Shen S Q 2014 *Phys. Rev. B* **90** 195404
[56] Liu D E and Baranger H U 2011 *Phys. Rev. B* **84** 201308
[57] Yan D D, Zhao S Y, Zhang Y B, Wang H X and Zang Z G 2022 *Opto-Electron. Adv.* **5** 200075
[58] Yang X, Lin Y, Wu T Z, *et al.* 2022 *Opto-Electron. Adv.* **5** 210123
[59] Thielmann A, Hettler M H, König J and Schön G 2005 *Phys. Rev. B* **71** 045341
[60] He X, Liu D L, Wang H F, *et al.* 2022 *Opto-Electron. Adv.* **5** 210015
[61] Aghassi J, Thielmann A, Hettler M H and Schön G 2006 *Phys. Rev. B* **73** 195323
[62] Chen J F and Li Z Y 2022 *Opto-Electron. Sci.* **1** 220001
[63] Elste F and Timm C 2006 *Phys. Rev. B* **73** 235305
[64] Weymann I, Bułka B R and Barnaś J 2011 *Phys. Rev. B* **83** 195302
[65] Koch J and von Oppen F 2005 *Phys. Rev. Lett.* **94** 206804
[66] Hübener H and Brandes T 2007 *Phys. Rev. Lett.* **99** 247206